Desalination and Water Treatment
www.deswater.com

doi: 10.5004/dwt.2017.21223

85 (2017) 226–236
August

Adsorptive removal of Direct Red-7 from aqueous solution by uncalcined and calcined zinc aluminium carbonate layered double hydroxide — kinetics and isotherm study

K. Manjula Rani*, P.N. Palanisamy

Centre for Environmental Research, Department of Chemistry, Kongu Engineering College, Perundurai, Erode 638 060, Tamil Nadu, India, emails: chemistrykmr@gmail.com (K. Manjula Rani), asppavithran@gmail.com (P.N. Palanisamy)

Received 27 December 2016; Accepted 14 July 2017

ABSTRACT

In this paper, two materials, namely zinc aluminium carbonate layered double hydroxide (ZAC-LDH) and calcined LDH (CZA-LDH) are prepared and employed for the removal of Direct Red-7 (DR-7) dye from aqueous solution. Batch mode studies are carried out for the removal of DR-7 using different parameters such as initial dye concentration, adsorbent dosage, contact time, temperature and pH. The adsorption kinetics is studied using classic equations of pseudo-first-order, pseudo-second-order and intraparticle diffusion models. The pseudo-second-order kinetic model fits well with the high correlation coefficient for the removal of DR-7 by both ZAC-LDH and CZA-LDH. The equilibrium data are examined using Langmuir and Freundlich isotherm models. The maximum adsorption capacity for the removal of DR-7 onto CZA-LDH is found to be 666.67 mg/g which is higher than the ZAC-LDH (357.14 mg/g) at 30°C. X-ray diffraction and Fourier transform infrared spectroscopy analysis also have been carried out to confirm the interaction of dye molecule onto the adsorbents. The evaluated thermodynamic parameters of $\Delta G°$ and $\Delta H°$ indicate that the adsorption process is spontaneous and endothermic in nature. The ZAC-LDH and CZA-LDH are thermally regenerated and reused for the dye removal of DR-7 from aqueous solution. The enhanced dye removal of DR-7 by CZA-LDH proves that the CZA-LDH is a more suitable adsorbent for the removal of DR-7 compared with ZAC-LDH from aqueous solution.

Keywords: Calcined layered double hydroxide; Direct Red-7; Isotherm; Memory effect; Kinetics; Thermodynamics

1. Introduction

Synthetic dyes play a major role in various industrial sectors like textile, dyeing houses, paper printers, leather and cosmetics. The effluents discharged from these industries and especially from textile industries carry a large number of dyes and other degraded products during the colouring process [1]. Even 1.0 mg/L of dye present in water is highly visible and undesirable that makes the water unfit for human consumption [2]. The release of colour in wastewater can affect the aquatic life in terms of hindering photosynthetic activity. Moreover, dyes are mutagenic and carcinogenic and they may cause severe damage such as dysfunction of the kidneys, reproductive system, liver, brain and central nervous system to human beings [3–5]. Therefore, various attempts are made for the removal of dyes from textile industry wastewater. Several methods are employed for the treatment of dyes and toxic molecules are generated from wastewater stream that includes coagulation, flocculation, precipitation [6], ozonation [7], oxidation [8], photocatalysis [9] and so on.

Adsorption is a widely used technique over the other methods for the removal of dyes because of its simple design and cost-effective operation [10]. Activated carbon is one such material used in adsorption process for the removal of dyes. Since it is an expensive material, there is an urgent need to investigate a low-cost adsorbent which is effective and economical. Some of the adsorbents prepared from waste

* Corresponding author.

materials such as orange peel, banana peel, lemon peel, egg shell, sawdust, rice husk, fly-ash, coir pith carbon, pomegranate peel, tea waste [11–16] and so on are alternative choices for activated carbon and employed as carbonaceous precursors for the removal of dyes from water and wastewater. Many researchers have reported the possibility of using activated carbon for the removal of dyes and other pollutants from aqueous solution. The wide spectrum of anionic pollutant present in wastewater treatment by using inorganic nanostructured layered double hydroxide (LDH) material attracts much interest among researcher. The possibility of the LDH material as adsorbent is attempted for treating the wastewater containing anionic dye pollutant like Direct Red-7 (DR-7).

LDHs are cheap and nontoxic materials that belong to the class of anionic clays [17]. The general formula of LDHs is $[M^{2+}_{1-x}M^{3+}_{x}(OH)_2]^{x+}(A^{n-})_{x/n}\cdot mH_2O$, where M^{2+} is divalent metal (Zn^{2+}, Mg^{2+}, Fe^{2+}, etc.), M^{3+} is trivalent metal (Al^{3+}, Fe^{3+}, etc.) and A^{n-} is interlayer anions (CO_3^{2-}, Cl^-, NO_3^-, SO_4^{2-}, etc.) [18,19]. Carbonates are the interlayer anion present in naturally occurring mineral hydroxide which is a member of this class of materials. LDH material shows a large flexibility of composition that can be made by using different nature of the divalent and trivalent cations in the layers, the type of interlayer anions (A^{n-}) and the stoichiometric coefficient (x) [20]. Due to the flexibility in composition and the exchangeability of interlayer anions, LDHs possess a wide variety of properties. These materials find wide applications in various fields, such as catalysis, adsorbents, ion exchanges, pharmaceutics, purification and so on [21–25]. Calcination of LDHs around 550°C destroys the layered structure of the clay and gives rise to porous mixtures of mixed oxides. Based on a unique property of LDHs, the so-called structural "memory effect", the layered structure of these clays can be reconstructed when the mixed oxides (calcined LDHs [CZA-LDH]) are exposed to aqueous solutions of anions. The anions used during the reconstruction process can be different from those of the original LDHs [26].

In the present study, nanostructured zinc aluminium carbonate LDH (ZAC-LDH) and its CZA-LDH are synthesized and employed as adsorbent for the removal of DR-7 from aqueous solution.

2. Materials and methods

2.1. Preparation of ZAC-LDH and CZA-LDH

ZAC-LDH is synthesized by using aqueous solution of $ZnSO_4.7H_2O$ and $Al_2(SO_4)_3.16H_2O$. The aqueous solution of zinc sulphate (1 M) and aluminium sulphate (1 M) are taken in the molar ratio $M^{2+}/M^{3+} = 3$ and mixed in magnetic stirrer. Exactly 0.3 g of the cetyltrimethylammonium bromide (CTAB) is added to the solution and it is made as a homogeneous mixture with a magnetic stirrer. The mixture of precipitating agent sodium hydroxide (1 M) and the intercalating carbonate anion source sodium carbonate (0.5 M) are added drop by drop until the pH is 9. The precipitate is poured into Teflon lined stainless steel autoclave and heated to about 120°C and maintained for about 8 h. The synthesized material is filtered, washed several times with double distilled water until the pH is neutral and dried at 80°C in hot air oven. The product obtained is named as ZAC-LDH. The calcined ZAC-LDH (CZA-LDH) is obtained by heating the original ZAC-LDH in a muffle furnace at 450°C for 2 h in an air atmosphere with heating and cooling rates of 10°C/min. Both the ZAC-LDH and the CZA-LDH samples are finely powdered and used for the analysis and adsorption studies.

2.2. Characterization

X-ray diffraction (XRD) pattern of both the samples are characterized by using a Shimadzu XRD-6000 diffractometer, with Ni-filtered Cu Kα radiation (λ = 1.54 Å) at 40 kV and 200 mA. Solid samples are mounted on alumina sample holder and basal spacing (d-spacing) is determined via powder technique. Sample scanning is done at 5°–80° range with a scanning rate of 1°/min. Similarly, the morphology of the samples before and after adsorption study is analyzed by using field emission scanning electron microscope (FESEM). The samples are coated with a gold/palladium film, and the FESEM images are obtained using a secondary electron detector. To investigate the interaction of functional group of the dye molecule onto the adsorbent, Fourier transform infrared spectroscopic (FTIR) spectra are recorded over the range of 400–4,000 cm^{-1} using FTIR spectrophotometer.

2.3. Preparation of the adsorbate solution

The dye used for the adsorption study is DR-7. Molecular formula of the dye is $C_{34}H_{26}N_6Na_2O_8S_2$ with colour index: 24100 and molecular weight: 756.72. The molecular structure of the dye is given in Fig. 1.

A stock solution of 1,000 mg/L is prepared by dissolving 1,000 mg of commercial DR-7 dye (purchased from local dye company) in 1,000 mL distilled water. The experimental solutions of the desired concentration 25, 50,75 and 100 mg/L of DR-7 are prepared from stock solutions. All the chemicals used throughout this study are of analytical grade reagents. Double distilled water is used for preparing all the solutions and reagents. The initial pH adjusted with 0.1 M HCl or 0.1 M NaOH is obtained by successive dilutions.

2.4. Batch adsorption experiments

The adsorption experiments are carried out with the two adsorbents prepared ZAC-LDH and CZA-LDH. The optimized dose 0.5 g/L of ZAC-LDH and 0.125 g/L of CZA-LDH (except dose variation study) used for different initial concentration of DR-7 are agitated in an Orbital shaker (REMI) at 170 rpm. The mixture is withdrawn at specified time intervals and centrifuged using electrical centrifuge (Universal)

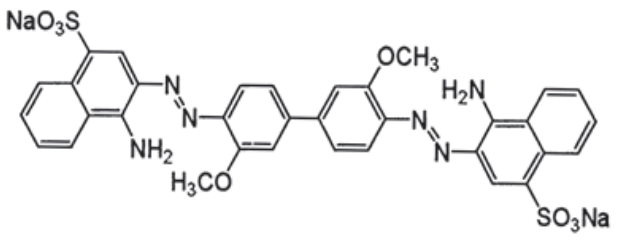

Fig. 1. Molecular structure of Direct Red-7.

at 5,000 rpm for 20 min. The unadsorbed supernatant liquid is analyzed for the residual dye concentration using Elico BL198 Bio spectrophotometer at λ_{max} 514 nm. The effect of pH study is made by using dilute HCl and NaOH solutions. The effect of temperature is also carried out at three different temperatures, that is, 30°C, 40°C and 45°C. All the experiments are carried out in duplicate for accuracy.

The amount of dye adsorbed at equilibrium (q_e) is calculated using the following equation:

$$q_e = (C_0 - C_e) \times \frac{V}{m} \quad (1)$$

where q_e is the quantity of dye adsorbed at equilibrium (mg/g), C_0 is the initial dye concentration (mg/L), C_e is the dye concentration at equilibrium (mg/L), V is the volume of the solution (L) and m is the mass of the ZAC-LDH/CZA-LDH sample (g).

2.5. Regeneration of the adsorbents

To check the reusability of the ZAC-LDH and CZA-LDH material for the removal of DR-7, calcination is carried out in a muffle furnace at 450°C for 2 h in an air atmosphere with heating and cooling rates of 10°C/min. Then, the thermally regenerated material is reused for the removal of DR-7 dye from aqueous solution with the same adsorbent dosage (0.5 g/L for ZAC-LDH and 0.125 g/L for CZA-LDH) for 100 mg/L initial dye concentration.

3. Results and discussion

3.1. Characterization

The X-ray diffractogram of the synthesized nanostructured ZAC-LDH fits well to the characteristic reflections of regular layered structure of LDH materials [27] is shown in Fig. 2(a) and its calcined product (CZA-LDH) is shown in Fig. 3(a). The occurrence of basal reflections of planes observed for ZAC-LDH resembles the previous study [28]. The synthesized material is highly crystalline inferred from the appearance of sharp peak at lower 2θ value. Secondary phases ZnO and $Al(OH)_3$ are also seen around the higher 2θ value in the range of 35°–60° along with brucite-like layer [29,30]. Since the interlayer distance between the layers in the synthesized ZAC-LDH is observed as 7.33 Å, it is known as a nanostructured material.

On calcination of ZAC-LDH at 450°C, the original layered structure is collapsed with the loss of interlayer carbonate anion, hydroxyl and water molecule with the formation of mixed metal oxide. The disappearance of basal reflections of planes (003) and (006) in XRD pattern in Fig. 3(a) confirms the loss of original layered structure with the formation of mixed metal oxides.

Figs. 2 and 3 give the XRD pattern of ZAC-LDH and CZA-LDH before and after dye adsorption. The dye adsorption by ZAC-LDH is mainly due to surface adsorption and slightly by intercalation which is shown in Fig. 4. This is confirmed by shifting basal reflection d(003) to lower 2θ value of 11.866° from 12.065° and it causes slight increase in interlayer distance between the metal ions from 7.330 to 7.458 Å compared with original ZAC-LDH [31]. The much higher uptake of dye by CZA-LDH is actually due to the reconstruction of the original LDH structure by intercalation of DR-7.

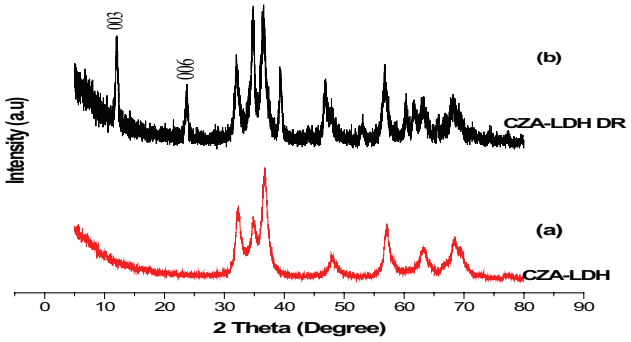

Fig. 3. XRD pattern of CZA-LDH (a) before adsorption and (b) after adsorption of dye DR-7.

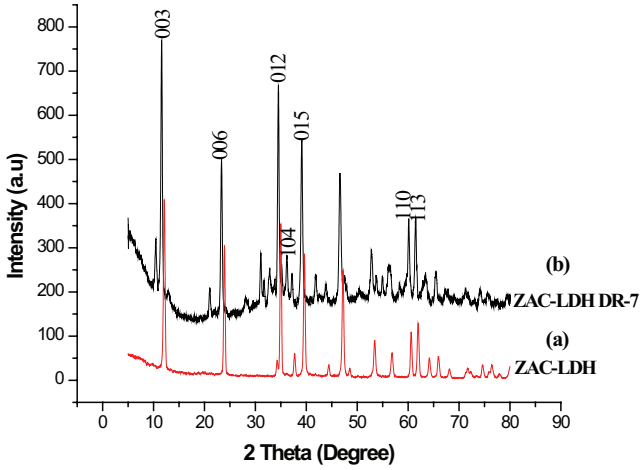

Fig. 2. XRD pattern of ZAC-LDH (a) before adsorption and (b) after adsorption of dye DR-7.

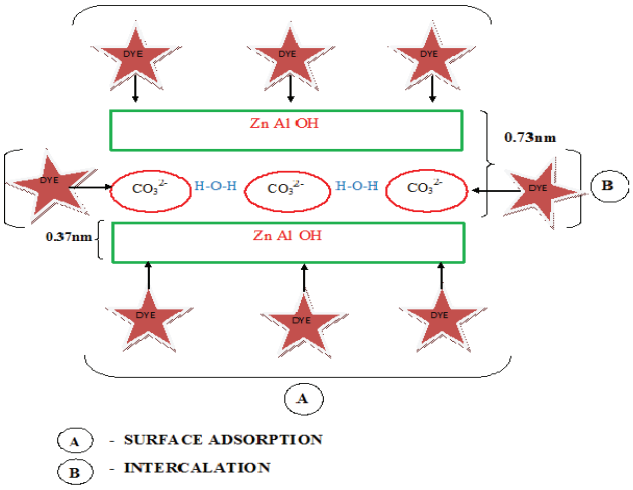

Fig. 4. Schematic representation of adsorption mechanism of DR-7 dye onto ZAC-LDH.

This is further evidenced by reappearance of basal reflections of plane *d*(003) and *d*(006) in Fig. 3(b). Thus, it proves the anion-exchange capacity of CZA-LDH with the anion of the DR-7 from wastewater.

FESEM images of ZAC-LDH and CZA-LDH before and after the adsorption of DR-7 are shown in Figs. 5 and 6(a) and (b). It is evidenced that the surface coverage and intrusion of the dye molecule in Figs. 5(b) and 6(b) prove the adsorption of DR-7 by both the adsorbents.

FTIR spectra of DR-7 and the dye adsorbed materials ZAC-LDH DR-7 and CZA-LDH DR-7 are shown in Figs. 7(a)–(c). The sulphonate (O=S–SO_3^-) stretching vibrations at 1,176 cm^{-1} and (S=O) group in 1,046 cm^{-1} appear in DR-7 matches with both the adsorbed material confirming the adsorption of DR-7 onto the adsorbents. The absorption band appears at 1,515 cm^{-1} corresponding to sulphonate group and at 700 cm^{-1} that corresponds to aromatic ring of dye molecule. Moreover, the intensity of the absorption peak at 1,360 cm^{-1} in Fig. 7(c) is lower than in Fig. 7(b) that supports the intercalation of anionic part of the dye molecule in the interlayer carbonate position through anion-exchange mechanism on the adsorbent CZA-LDH.

3.2. *Effect of agitation time and initial dye concentration*

To determine the rate of adsorption, experiments are conducted at different initial dye concentrations ranging from 25 to 100 mg/L at 30°C. It is observed that the adsorption capacity at equilibrium (q_e) is increased while increasing the concentration of the dye solution. This is mainly due to an increase in the availability of dye molecule over the active sites on the adsorbents [32]. The maximum amount of 650 and 164.5 mg/g of dye is adsorbed within the contact time of 40 min by CZA-LDH and ZAC-LDH, respectively. After this both the curves reach equilibrium at 60 min and continue with no significant change

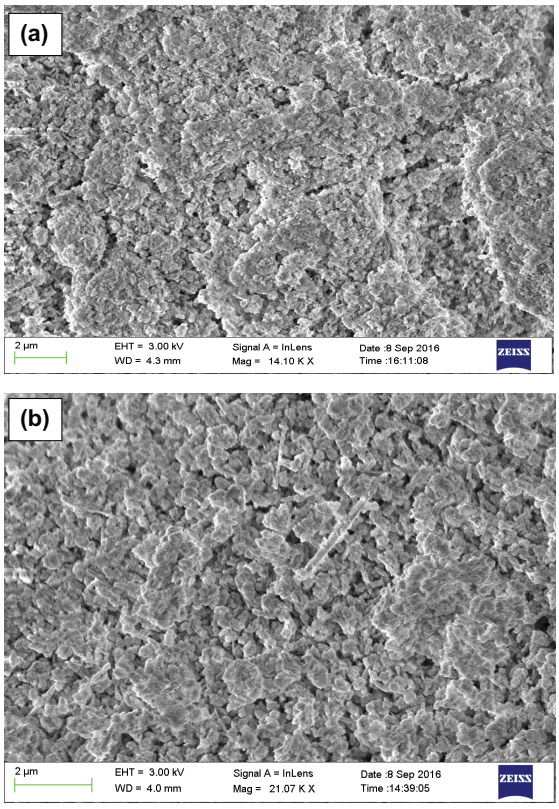

Fig. 5. FESEM image of ZAC-LDH (a) before adsorption of DR-7 and (b) after adsorption of DR-7.

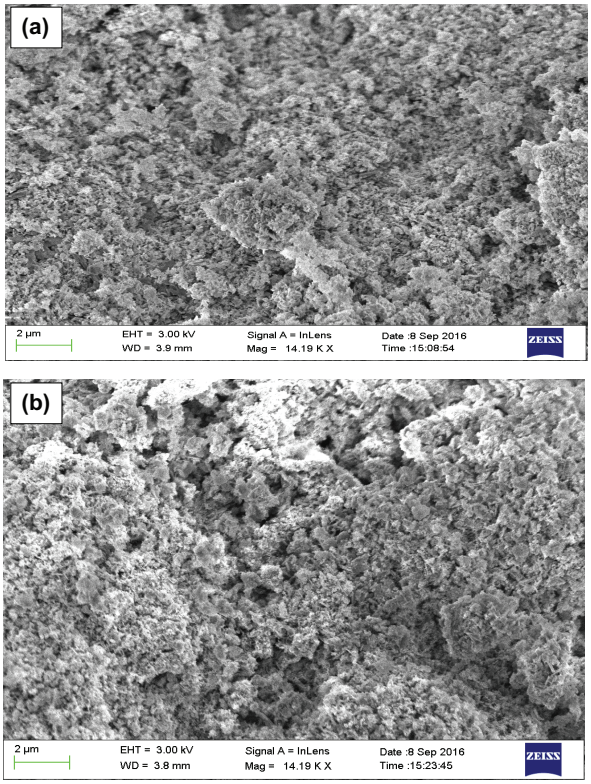

Fig. 6. FESEM image of CZA-LDH (a) before adsorption of DR-7 and (b) after adsorption of DR-7.

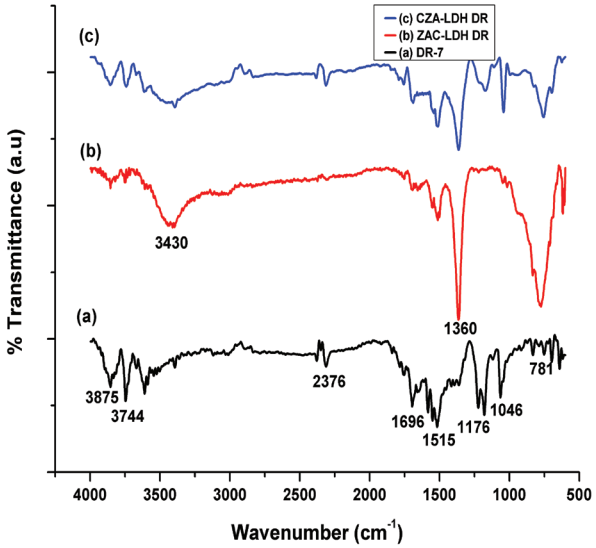

Fig. 7. FTIR spectra of (a) Direct Red-7, (b) ZAC-LDH DR-7 and (c) CZA-LDH DR-7.

in the extent of adsorption. The percentage removal of dye decreases from 100% to 85.42% for CZA-LDH and from 96.15% to 88.79% for ZAC-LDH while increasing the initial dye concentrations from 25 to 100 mg/L as shown in Fig. 8. This shows that the adsorption is highly dependent on initial concentration of dye. The reason is that at lower concentration, the available surface area is more when compared with high concentration. However, at high concentration, the available site of adsorption becomes lesser and hence the percentage removal of dye gets decreased with an increase in initial dye concentration.

3.3. Effect of temperature

To investigate the effect of temperature for the removal of DR-7 by ZAC-LDH and CZA-LDH, the experiments are carried out at three different temperatures 30°C, 40°C and 50°C. From the results, it is observed that the percentage of DR-7 removal is increased from 88.79% to 94.50% by ZAC-LDH and from 85.42% to 92.71% by CZA-LDH on increasing the temperature. This proves that the sorption of direct dye onto both adsorbents is endothermic.

3.4. Effect of pH

The effect of pH on the adsorption of DR-7 by ZAC-LDH and CZA-LDH is investigated by varying the initial pH of dye (concentration of dye 100 mg/L) between 4 and 12 as the original colour of the dye gets changed below pH 4. The point zero charge (PZC) of adsorbent is an important one to explain the effect of pH for the dye removal. The PZC of ZAC-LDH and CZA-LDH are determined by following the procedure [33] which is found to be 8.07 and 8.6, respectively. The percentage of dye removal by ZAC-LDH and CZA-LDH is increased at pH < PZC and decreased at pH > PZC. At pH < PZC, high concentration of H^+ in the dye solution results in the positive charge on both the LDH surface that causes electrostatic attraction between anionic dye and positively charged LDH surface causes increase in the percentage of dye removal, whereas at pH > PZC, the electrostatic repulsion of deprotonated adsorbent of ZAC-LDH and CZA-LDH surface and dye anion decreases the rate of adsorption. Fig. 9 clearly shows that the maximum dye removal of 95.6% and 100% for ZAC-LDH and CZA-LDH is observed in the acidic pH between 3 and 6.

3.5. Effect of adsorbent dose

The effect of adsorbent dose for the removal of DR-7 by ZAC-LDH and CZA-LDH is tested with 100 mg/L initial dye concentration. Figs. 10(a) and (b) show the maximum dye removal of 90.65% by ZAC-LDH with the adsorbent dose of 0.5 g/L and 88.79% by CZA-LDH with minimal increment of adsorbent 0.125 g/L. After this there is no significant change in the dye removal because of the attainment of equilibrium between both the adsorbent ZAC-LDH and CZA-LDH and dye molecule.

3.6. Kinetic studies

3.6.1. Pseudo-first-order model

In this study, the adsorption of DR-7 dye by ZAC-LDH and CZA-LDH are analyzed using pseudo-first-order, pseudo-second-order and intraparticle diffusion models. Pseudo-first-order kinetic model assumes that the rate of change of solute uptake with time is directly proportional to the

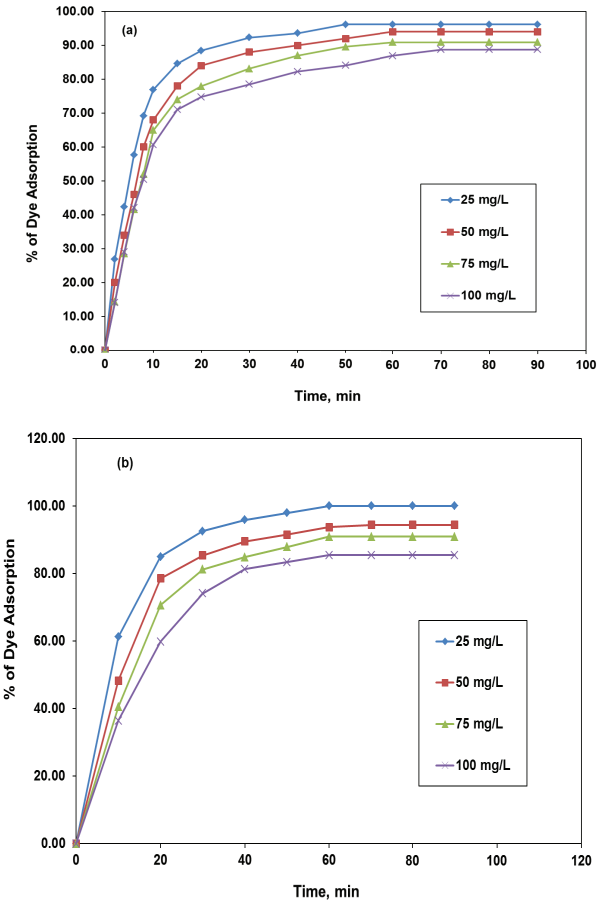

Fig. 8. Effect of initial dye concentration on the adsorption of DR-7 by (a) ZAC-LDH and (b) CZA-LDH.

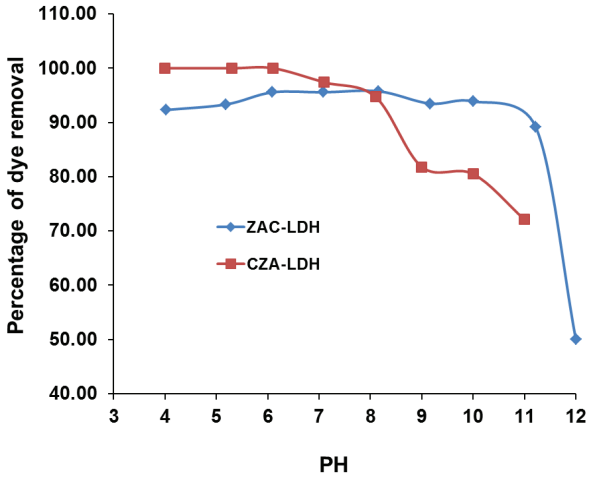

Fig. 9. Effect of pH on the removal of DR-7 dye by ZAC-LDH and CZA-LDH (initial concentration 100 ppm; temperature 30°C).

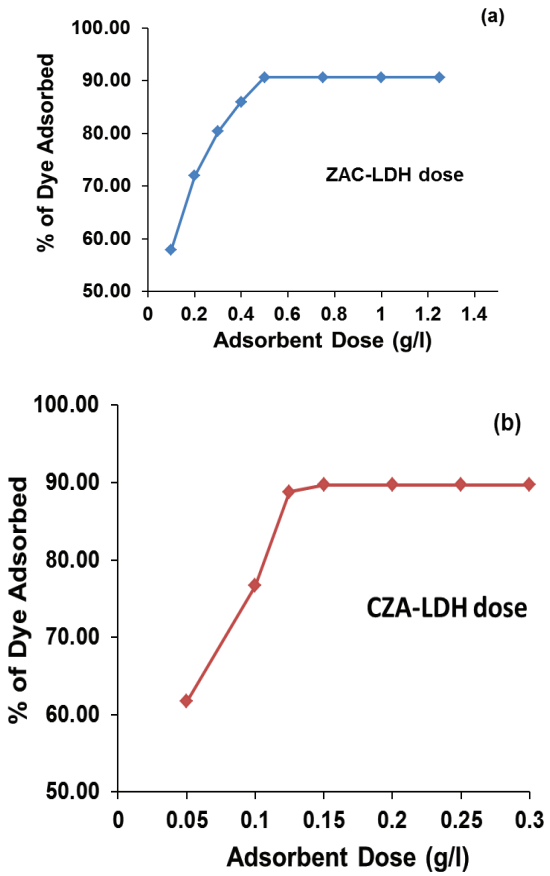

Fig. 10. The effect of adsorbent dose for the removal of DR-7 dye by (a) ZAC-LDH and (b) CZA-LDH (initial concentration 100 ppm; temperature 30°C).

difference in solution concentration and the amount of solid uptake. The pseudo-first-order rate equation proposed by Lagergren [34] is as follows:

$$\log(q_e - q_t) = \log q_e - \left(\frac{k_1}{2.303}\right)t \quad (2)$$

where q_e and q_t are the amount of dye adsorbed at equilibrium and time t (min), k_1 is the pseudo-first-order rate constant (min^{-1}). The value of q_e and k_1 is calculated from the intercept and the slope of the plot $\log(q_e - q_t)$ vs. time for different initial concentrations and different temperatures for both the adsorbents. The values calculated are summarized in Tables 1(a) and (b). The pseudo-first-order kinetic model of Lagergren does not fit well with the experimental data over the whole range of initial concentrations studied. Similar results are observed for the adsorption of Congo red by chitosan hydrogel beads impregnated with CTAB [35].

3.6.2. Pseudo-second-order model

The pseudo-second-order kinetic equation is expressed as:

$$\frac{t}{q_t} = \frac{1}{k_2 q_e^{\,2}} + \frac{1}{q_e}t \quad (3)$$

The values of k_2 pseudo-second-order rate constant (g/mg min) and q_e equilibrium adsorption capacity (mg/g) can be calculated from the intercept and the slope of the plot between t/q_t vs. t for different initial concentrations (shown in Figs. 11(a) and (b)) and temperature. The pseudo-second-order kinetic parameters calculated are given in Tables 1(a) and (b). The calculated rate constant k_2 value decreases with the increase in the initial dye concentration. This trend is observed due to the decrease in the available active sites on the adsorbent for the dye adsorption. The adsorption of DR-7 onto ZAC-LDH and CZA-LDH fits well with the pseudo-second-order kinetics than the pseudo-first-order kinetic model with high correlation coefficient (R^2) for all the concentrations.

3.6.3. Intraparticle diffusion model

It is important to determine the rate-determining step in adsorption studies. Since the particles are vigorously agitated during the experiment, there is a possibility to transport the adsorbate ion from the solution into the pores of adsorbent which is the rate-limiting step. The pseudo-first-order and pseudo-second-order kinetic models cannot identify the diffusion mechanism. Then, the kinetic results are analyzed by using the intraparticle diffusion model to elucidate the diffusion mechanism. The intraparticle diffusion model is expressed as:

$$q_t = k_{id}\, t^{1/2} + C \quad (4)$$

where k_{id} is the intraparticle rate constant ($mg/g/min^{1/2}$) and q_t is the amount of dye adsorbed at time t (mg/g). The intraparticle diffusion model is tested by plotting a graph between the amount of dye adsorbed q_t and $t^{½}$ at different time intervals for different concentrations as shown in Figs. 12(a) and (b). The values of k_{id} for all the concentrations at 30°C and for different temperatures for 100 mg/L initial dye concentration are determined from the slopes of plots and presented in Tables 1(a) and (b). Since the plot is not linear to the whole time range and not passed through the origin, it is implied that the adsorption of DR-7 by ZAC-LDH and CZA-LDH follow the boundary layer diffusion to some extent and not to the whole range [36].

3.7. Adsorption isotherm

Adsorption isotherm is an important parameter to analyze the equilibrium relation between the adsorbate in the liquid phase and the adsorbate adsorbed on the surface of the adsorbent at constant temperatures. In this study, Langmuir [37] and Freundlich [38] isotherm models are used to analyze the adsorption equilibrium of DR-7 by ZAC-LDH and CZA-LDH.

3.7.1. Langmuir isotherm

The Langmuir adsorption isotherm is the best known linear model for monolayer adsorption on the homogeneous surface and the most frequently utilized isotherm to determine the adsorption parameters. Langmuir model is represented by the following equation:

Table 1(a)
Kinetic parameters for the adsorption of direct dye DR-7 by ZAC-LDH and CZA-LDH for different initial dye concentration at temperature 30°C

Adsorbents	ZAC-LDH				CZA-LDH			
	Initial concentration (mg/L)							
Parameter	25	50	75	100	25	50	75	100
q_e experimental (mg/g)	48.08	94.00	136.36	177.57	200.00	377.60	545.45	683.33
	Pseudo-first-order kinetic model							
k_1 (min^{-1})	0.081	0.076	0.080	0.059	0.067	0.071	0.069	0.076
q_e calculated (mg/g)	32.90	68.79	114.87	128.91	168.42	336.28	535.92	802.23
R^2	0.9432	0.9607	0.9808	0.9587	0.9899	0.9855	0.9933	0.9917
	Pseudo-second-order kinetic model							
k_2 (g/mg min)	0.005	0.002	0.001	0.001	0.0008	0.0003	0.0001	0.0001
h	12.920	17.094	19.763	24.814	38.314	52.356	58.480	62.893
q_e calculated (mg/g)	50.76	102.04	151.52	196.08	217.39	416.67	625.00	833.33
R^2	0.999	0.9981	0.9957	0.9972	0.9986	0.9961	0.9922	0.9898
	Intraparticle diffusion model							
k_{id} (mg/g/$min^{½}$)	0.291	0.127	0.081	0.063	0.041	0.024	0.018	0.239
R^2	0.7035	0.76	0.7759	0.8	0.7281	0.7539	0.787	0.9743

Table 1(b)
Kinetic parameters for the adsorption of direct dye DR-7 by ZAC-LDH and CZA-LDH at different temperatures (initial dye concentration of 100 mg/L)

Adsorbents	ZAC-LDH			CZA-LDH		
	Temperature (°C)					
Parameter	30	40	50	30	40	50
q_e experimental (mg/g)	177.57	183.49	188.99	683.33	716.67	741.67
	Pseudo-first-order kinetic model					
k_1 (min^{-1})	0.059	0.073	0.087	0.076	0.074	0.081
q_e calculated (mg/g)	128.91	138.96	149.83	802.23	754.57	723.10
R^2	0.9587	0.9856	0.9884	0.9917	0.9978	0.9925
	Pseudo-second-order kinetic model					
k_2 (g/mg min)	0.00065	0.00080	0.00092	0.00009	0.00012	0.00018
H	24.814	31.847	38.314	62.893	83.333	123.457
q_e calculated (mg/g)	196.08	200.00	204.08	833.33	833.33	833.33
R^2	0.9972	0.9988	0.999	0.9898	0.9957	0.9981
	Intraparticle diffusion model					
k_{id} (mg/g/$min^{½}$)	0.063	0.065	0.066	0.018	0.020	0.024
R^2	0.8	0.7904	0.7737	0.787	0.7907	0.7649

$$\frac{C_e}{q_e} = \frac{1}{Q_0.b_L} + \frac{C_e}{Q_0} \quad (5)$$

where C_e is the equilibrium concentration of the adsorbate (mg/L), q_e is the amount of adsorbate adsorbed per unit mass of adsorbent (mg/g), Q_0 and b_L are constants related to monolayer adsorption capacity and energy of adsorption (L/mg). Langmuir dimensionless constant R_L value indicates the adsorption nature to be either unfavourable if $R_L > 1$, linear if $R_L = 1$, favourable if $0 < R_L < 1$ and irreversible if $R_L = 0$. From the calculated value in Table 2, the R_L value is in between 0 and 1 indicating that the adsorption is favourable. The plot of C_e/q_e against C_e gives a straight line with slope $1/Q_0$ and intercept with b. The maximum monolayer coverage capacity (Q_0) from Langmuir Isotherm model is found to be 357.14 and 666.67 mg/g at 30°C for ZAC-LDH and CZA-LDH, respectively.

3.7.2. Freundlich model

The Freundlich isotherm is an empirical equation employed to describe the multilayer adsorption and adsorption on heterogeneous systems. The linearized form of Freundlich equation can be written as:

$$\log q_e = \log k_f + \frac{1}{n}\log C_e \quad (6)$$

where k_f is the measure of adsorption capacity and n is the adsorption intensity and these are calculated from the intercept and the slope of a linear plot of $\log q_e$ vs. $\log C_e$ as shown in Fig. 13. The value of $1/n$ is lower than one for the adsorption of DR-7 dye onto ZAC-LDH and CZA-LDH indicating that the adsorption of DR-7 by both the adsorbent materials is favourable. Moreover, equilibrium data fit well to the Freundlich isotherm with high correlation coefficient value (R^2). The much higher correlation coefficients value for the Freundlich isotherm predicts heterogeneity and multilayer adsorption of DR-7 by both the adsorbents shown in Table 2.

3.8. Thermodynamic parameters

Thermodynamic parameters such as Gibb's free energy change ($\Delta G°$), enthalpy change ($\Delta H°$) and entropy change ($\Delta S°$) of adsorption are calculated from the binding constant obtained from Langmuir equation using the following equations as given in Table 3.

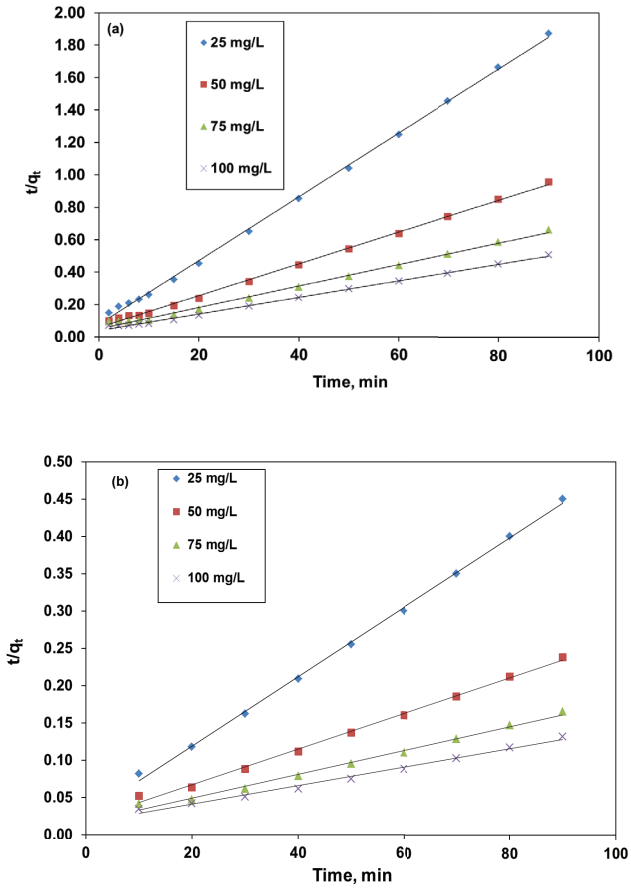

Fig. 11. Pseudo-second-order kinetic model for the removal of DR-7 by (a) ZAC-LDH and (b) CZA-LDH.

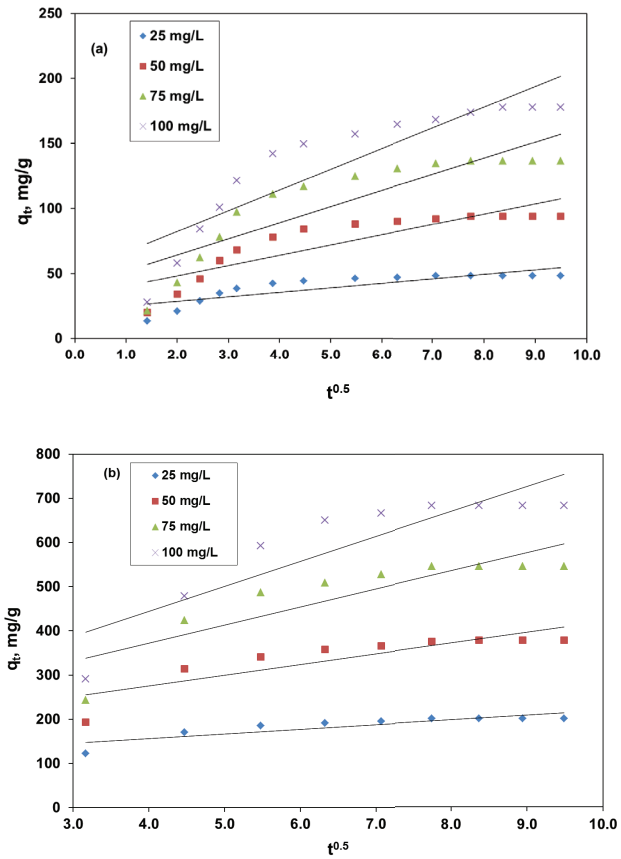

Fig. 12. Intraparticle diffusion model for the removal of DR-7 by (a) ZAC-LDH and (b) CZA-LDH.

Table 2
Isotherm parameters for adsorption of DR-7 by ZAC-LDH and CZA-LDH

Sample	Temperature (°C)	Isotherm models						
		Langmuir				Freundlich		
		Q_0	b	R_L	R^2	n	k_f	R^2
ZAC-LDH	30	357.14	0.0051	0.7969	0.8431	1.331	22.387	0.9912
	40	263.16	0.0073	0.7332	0.9573	1.829	48.217	0.992
	50	277.78	0.0069	0.7425	0.9599	1.065	31.601	0.9845
CZA-LDH	30	666.67	0.01157	0.6336	0.959	3.028	225.320	0.9889
	40	714.29	0.0109	0.6472	0.9653	2.670	223.254	0.9832
	50	714.29	0.0110	0.6450	0.9837	3.423	303.319	0.9819

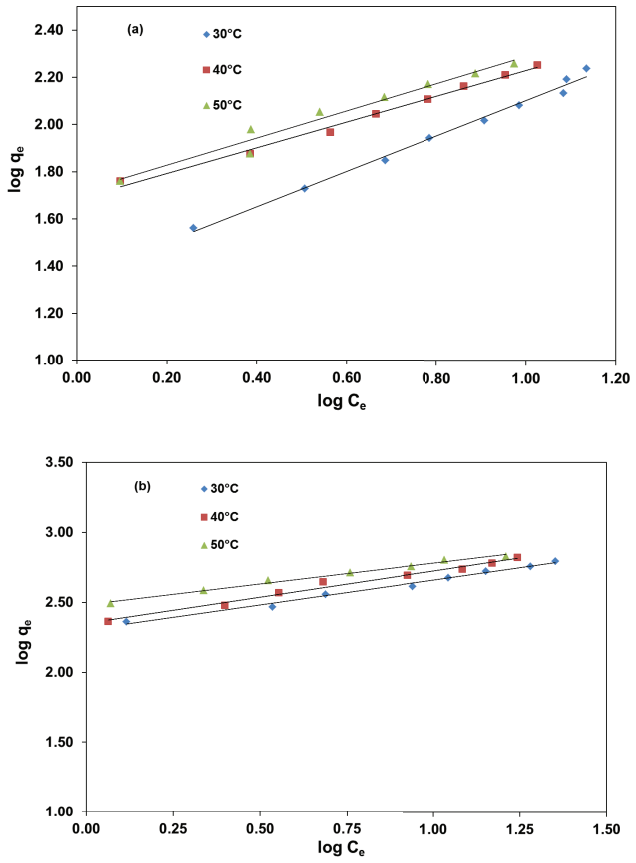

Fig. 13. Freundlich isotherms for adsorption of DR-7 by (a) ZAC-LDH and (b) CZA-LDH.

Table 3
Thermodynamic parameters from Van't Hoff plots for the adsorption of direct dye DR-7 by ZAC-LDH and CZA-LDH at different temperature

Adsorbent	Temperature (°C)	$\Delta G°$ (kJ/mol)	$\Delta H°$ (kJ/mol)	$\Delta S°$ (J/K/mol)
ZAC-LDH	30	–5.21	31.45	120.84
	40	–6.27		
	50	–7.64		
CZA-LDH	30	–4.45	31.52	118.67
	40	–5.60		
	50	–6.83		

$$\Delta G° = -RT \ln K_c \quad (7)$$

$$\ln K_c = \frac{\Delta S°}{R} - \frac{\Delta H°}{RT} \quad (8)$$

The $\Delta H°$ values are calculated from the slopes of linear variation of ln$K$ vs. 1/T. The negative value of $\Delta G°$ indicates the high affinity of DR-7 dye to the surface of ZAC-LDH and CZA-LDH and demonstrates that the adsorption is favourable and spontaneous in nature.

The positive value $\Delta H°$ calculated for both the adsorbents ZAC-LDH and CZA-LDH for the adsorption of DR-7 dye is an endothermic process which is supported by the increase in the adsorption of the dye with the increase in temperature. Furthermore, the positive $\Delta S°$ values indicate that the degree of freedom gets increased at the solid–liquid interface during adsorption of the direct dye. The enthalpy value $\Delta H°$ is used to distinguish between the chemical and physical adsorption [39,40]. The enthalpy change value ($\Delta H°$) observed for the removal of dye by both adsorbents is below 40 kJ/mol supporting the nature of the adsorption process to be physisorption [41]. All the values in Table 3 are in good agreement with previous studies reported for the removal of anionic dyes with LDH materials [42–44].

3.9. Reusability of the adsorbents

To analyze the reusability of the adsorbent, thermal regeneration is carried out in a muffle furnace at 450°C for 2 h in an air atmosphere with heating and cooling rates of 10°C/min for each cycle. The regenerated material is used for the removal of DR-7 dye from aqueous solution with the same adsorbent dosage (0.5 g/L for ZAC-LDH and 0.125 g/L for CZA-LDH) for 100 mg/L initial dye concentration. Three regeneration cycles are performed to understand the efficiency and reusability of the materials for the removal of DR-7 from aqueous solution. In the first cycle, 7.47% of increase and 6.55% of decrease in the removal of DR-7 are observed for ZAC-LDH and CZA-LDH, respectively. The increase of percentage removal in first cycle by ZAC-LDH may be due to loss and reconstruction of original LDH structure by the intercalation of dye molecule. On successive cycle, there is a decrease in the removal by both the adsorbents ZAC-LDH and CZA-LDH observed as 85.05% and 72.9% (second cycle) and 75.70% and 57.01% (third cycle), respectively, for the removal of DR-7 from aqueous solution.

4. Conclusion

In this study, the adsorption behaviour of synthesized ZAC-LDH and CZA-LDH is examined for the removal of DR-7 dye from aqueous solution. The amount of adsorption of DR-7 gets increased from 48.08 to 177.57 mg/g for ZAC-LDH and from 200 to 683.33 mg/g for CZA-LDH with an increase in the initial concentrations from 25 to 100 mg/L. The results obtained from the studies reveal that the pseudo-second-order kinetic model and Freundlich isotherm models are more appropriate for the DR-7 dye uptake by ZAC-LDH and CZA-LDH with heterogeneity and multilayer adsorption. The maximum Langmuir adsorption capacity (Q_0) from Langmuir isotherm model is found to be 357.14 and 666.67 mg/g at 30°C for ZAC-LDH and CZA-LDH, respectively. The XRD pattern and FTIR spectra substantiate the adsorption of DR-7 onto ZAC-LDH and CZA-LDH. Acidic pH preferably below 7 influences much the removal of DR-7 dye by both the adsorbents. The negative value of $\Delta G°$ and positive value of $\Delta H°$ indicate that the adsorption process is spontaneous and endothermic in nature. Endothermic nature is further evidenced by the increase in the adsorption of the dye with the increase in temperature. From the results,

it is clear that the CZA-LDH is a more suitable adsorbent than the ZAC-LDH for the removal of high concentration of DR-7 dye from aqueous solution.

Acknowledgements

The authors gratefully acknowledge the financial support provided by the University Grants Commission (UGC), New Delhi under the Minor Research Project scheme (Project Proposal Number: 1161) to carry out the present research.

References

[1] C. Wang, A. Yediler, D. Linert, Z. Wang, A. Kettrup, Toxicity evaluation of reactive dyestuffs, auxiliaries and selected effluents in textile finishing industry to luminescent bacteria *Vibrio fischeri*, Chemosphere, 46 (2002) 339–344.
[2] R. Malik, D.S. Ramteke, S.R. Wate, Adsorption of malachite green on groundnut shell waste based powdered activated carbon, Waste Manage., 27 (2007) 1129–1138.
[3] K. Kadirvelu, M. Kavipriya, C. Karthika, M. Radhika, N. Vennilamani, S. Pattabhi, Utilization of various agricultural wastes for activated carbon preparation and application for the removal of dyes and metal ions from aqueous solutions, Bioresour. Technol., 87 (2003) 129–132.
[4] A.R. Dinçer, Y. Güneş, N. Karakaya, E. Güneş, Comparison of activated carbon and bottom ash for removal of reactive dye from aqueous solution, Bioresour. Technol., 98 (2007) 834–839.
[5] D. Shen, J. Fan, W. Zhou, B. Gao, Q. Yue, Q. Kang, Adsorption kinetics and isotherm of anionic dyes onto organo-bentonite from single and multisolute systems, J. Hazard. Mater., 172 (2009) 99–107.
[6] P. Pandit, S. Basu, Removal of organic dyes from water by liquid–liquid extraction using reverse micelles, J. Colloid Interface Sci., 245 (2002) 208–214.
[7] M. Khadhraoui, H. Trabelsi, M. Ksibi, S. Bouguerra, B. Elleuch, Discoloration and detoxicification of a Congo red dye solution by means of ozone treatment for a possible water reuse, J. Hazard. Mater., 161 (2009) 974–981.
[8] N. Jagtap, V. Ramaswamy, Oxidation of aniline over titania pillared montmorillonite clays, Appl. Clay Sci., 33 (2006) 89–98.
[9] M.N. Chong, B. Jin, C.W. Chow, C.P. Saint, A new approach to optimise an annular slurry photoreactor system for the degradation of Congo Red: statistical analysis and modeling, Chem. Eng. J., 152 (2009) 158–166.
[10] M. Mohammod, T.K. Sen, S. Maitra, B.K. Dutta, Removal of Zn^{2+} from aqueous solution using castor seed hull, Water Air Soil Pollut., 215 (2011) 609–620.
[11] G. Annadurai, R.S. Juang, D.J. Lee, Use of cellulose-based wastes for adsorption of dyes from aqueous solutions, J. Hazard. Mater., 92 (2002) 263–274.
[12] A. Mittal, A. Malviya, D. Kaur, J. Mittal, L. Kurup, Studies on the adsorption kinetics and isotherms for the removal and recovery of Methyl Orange from wastewaters using waste materials, J. Hazard. Mater., 148 (2007) 229–240.
[13] K.V. Kumar, Optimum sorption isotherm by linear and non-linear methods for malachite green onto lemon peel, Dyes Pigm., 74 (2007) 595–597.
[14] K. Kadirvelu, C. Namasivayam, Agricultural by-product as metal adsorbent: sorption of lead(II) from aqueous solution onto coirpith carbon, Environ. Technol., 21 (2000) 1091–1097.
[15] M. Jambulingam, N. Renugadevi, S. Karthikeyan, J. Kiruthika, Adsorption of Cr(VI) from aqueous solution using a low cost activated carbon prepared from pomegranate peel, Nat. Environ. Pollut. Technol., 6 (2007) 15–22.
[16] K. Manjula Rani, P.N. Palanisamy, S. Gayathri, S. Tamilselvi, Adsorptive removal of basic Violet dye form aqueous solution by activated carbon prepared from tea dust material, Int. J. Innovative Res. Sci. Eng. Technol., 4 (2015) 6845–6853.
[17] F. Cavani, F. Trifirò, A. Vaccari, Hydrotalcite-type anionic clays: preparation, properties and applications, Catal. Today, 11 (1991) 173–301.
[18] S.V. Prasanna, P.V. Kamath, Chomate uptake characteristics of the pristine layered double hydroxides of mg with Al, Solid State Sci., 10 (2008) 260–266.
[19] D.G. Evance, X. Duan, Preparation of layered double hydroxides and their applications as additives in polymers, as precursors to magnetic materials and in biology and medicine, Chem. Commun., 5 (2006) 485–496.
[20] P. Benito, F.M. Labajos, J. Rocha, V. Rives, Influence of microwave radiation on the textural properties of layered double hydroxides, Microporous Mesoporous Mater., 94 (2006) 148–158.
[21] M.O. Adebajo, R.L. Frost, Oxidative benzene methylation with methane over MCM-41 and zeolite catalysts: effect of framework aluminum, SiO_2/Al_2O_3 ratio, and zeolite pore structure, Energy Fuels, 19 (2005) 783–790.
[22] K. Grover, S. Komarneni, H. Katsuki, Uptake of arsenite by synthetic layered double hydroxides, Water Res., 43 (2009) 3884–3890.
[23] N. Iyi, K. Tamura, H. Yamada, One-pot synthesis of organophilic layered double hydroxides (LDHs) containing aliphatic carboxylates: extended "homogeneous precipitation" method, J. Colloid Interface Sci., 340 (2009) 67–73.
[24] J.H. Choy, S.J. Choi, J.M. Oh, T. Park, Clay minerals and layered double hydroxides for novel biological applications, Appl. Clay Sci., 36 (2007) 122–132.
[25] H. Zhao, K.L. Nagy, Dodecyl sulfate–hydrotalcite nanocomposites for trapping chlorinated organic pollutants in water, J. Colloid Interface Sci., 274 (2004) 613–624.
[26] S. Britto, A.V. Radha, N. Ravishankar, P.V. Kamath, Solution decomposition of the layered double hydroxide (LDH) of Zn with Al, Solid State Sci., 9 (2007) 279–286.
[27] S. Miyata, The syntheses of hydrotalcite-like compounds and their structures and physico-chemical properties I: the systems Mg^{2+}-Al^{3+}-NO_3^-, Mg^{2+}-Al^{3+}-Cl^-, Mg^{2+}-Al^{3+}-ClO_4^-, Ni^{2+}-Al^{3+}-Cl^- and Zn^{2+}-Al^{3+}-Cl, Clays Clay Miner., 23 (1975) 369–375.
[28] Z.P. Xu, G.Q. Lu, Hydrothermal synthesis of layered double hydroxides (LDHs) from mixed MgO and Al_2O_3: LDH formation mechanism, Chem. Mater., 17 (2005) 1055–1062.
[29] D. Carriazo, M. Del Arco, E. Garcia-Lopez, G. Marci, C. Martin, L. Palmisano, V. Rives, Zn,Al hydrotalcites calcined at different temperatures: preparation, characterization and photocatalytic activity in gas–solid regime, J. Mol. Catal. A: Chem., 342 (2011) 83–90.
[30] F.L. Theiss, M.J. Sear-Hall, S.J. Palmer, R.L. Frost, Zinc aluminium layered double hydroxides for the removal of iodine and iodide from aqueous solutions, Desal. Wat. Treat., 39 (2012) 166–175.
[31] F.P. de Sá, B.N. Cunha, L.M. Nunes, Effect of pH on the adsorption of Sunset Yellow FCF food dye into a layered double hydroxide (CaAl-LDH-NO_3), Chem. Eng. J., 215–216 (2013) 122–127.
[32] Z. Aksu, Ş.Ş. Çağatay, Investigation of biosorption of Gemazol Turquise Blue-G reactive dye by dried *Rhizopus arrhizus* in batch and continuous systems, Sep. Purif. Technol., 48 (2006) 24–35.
[33] Y.C. Sharma, V. Srivastava, C.H. Weng, S.N. Upadhyay, Removal of Cr (VI) from wastewater by adsorption on iron nanoparticles, Can. J. Chem. Eng., 87 (2009) 921–929.
[34] S. Lagergren, About the theory of so-called adsorption of soluble substances, K. Sven. Vetensk.akad. Handl., 24 (1898) 1–39.
[35] S. Chattergee, D.S. Lee, M.W. Lee, S.H. Woo, Enhanced adsorption of congo red from aqueous solutions by chitosan hydrogel beads impregnated with cetyl trimethyl ammonium bromide, Bio. Res. Technol., 100 (2009) 2803–2809.
[36] W.H. Cheung, Y.S. Szeto, G. McKay, Intraparticle diffusion processes during acid dye adsorption onto chitosan, Bioresour. Technol., 98 (2007) 2897–2904.
[37] I. Langmuir, The adsorption of gases on plane surfaces of glass, mica and platinum, J. Am. Chem. Soc., 40 (1918) 1361–1403.
[38] H.M.F. Freundlich, Over the adsorption in solution, J. Phys. Chem., 57 (1906) 1100–1107.

[39] J. Budhraja, M. Singh, Spectrophotometric study of adsorption of bromo thymol blue on charcoal and phosphates of FeIII, AlIII, CrIII and ZnII, J. Indian Chem. Soc., 81 (2004) 573–575.
[40] M. Doula, A. Ioannou, A. Dimirkou, Thermodynamics of copper adsorption-desorption by Ca-Kaolinite, Adsorption, 6 (2000) 325–335.
[41] M.M. Bouhent, Z. Derriche, R. Denoyel, V. Prevot, C. Forano, Thermodynamical and structural insights of orange II adsorption by Mg_RAlNO_3 layered double hydroxides, J. Solid State Chem., 184 (2011) 1016–1024.
[42] R. Marangoni, M. Bouhent, C. Taviot-Guého, F. Wypych, F. Leroux, Zn_2Al layered double hydroxides intercalated and adsorbed with anionic blue dyes: a physico-chemical characterization, J. Colloid Interface Sci., 333 (2009) 120–127.
[43] Z.M. Ni, S.J. Xia, L.G. Wang, F.F. Xing, G.X. Pan, Treatment of methyl orange by calcined layered double hydroxides in aqueous solution: adsorption property and kinetic studies, J. Colloid Interface Sci., 316 (2007) 284–291.
[44] N.B.H. Abdelkader, A. Bentouami, Z. Derriche, N. Bettahar, L.C. De Menorval, Synthesis and characterization of Mg–Fe layer double hydroxides and its application on adsorption of Orange G from aqueous solution, Chem. Eng. J., 169 (2011) 231–238.